

# Experimental Rotordynamics and Flow Visualization Approach for Periodically Reversed Flows of a Francis-Type Pump-Turbine in Generating Mode at Off-Design Operating Conditions

---

PROYECTO DE GRADO

PARA LA OBTENCIÓN DEL TÍTULO DE MAGISTER EN  
INGENIERÍA

POR

Sebastián Guzmán Díaz



Medellín  
2011



# Introduction

---

The flow instability phenomena in the turbo machinery are a long standing problem of widely research and application. There are several sources of flow disturbances that might cause flow instabilities found in the rotor vibration signals resulting in several responses of rotor to different kinds of excitation. These instabilities, in this case rotating-stall (RS), can cause critical operating conditions with strong dynamic loading on the machines. Earlier investigations point out that RS phenomenon is still obscure and that further research is necessary to reveal its flow dynamics.

This project presents a series of experiments designed to investigate the fluid mechanism and behavior of RS phenomenon. This unsteady stalling behavior was studied in a reduced scale pump-turbine model in generating mode instrumented with flow pressure measurements, proximity probes, keyphasor signal, and high speed tuft visualization; also, specific image processing techniques were performed to investigate the flow and rotor dynamic at operating points under RS condition.

The overall goal is to understand the fluid dynamic processes that lead to RS phenomena and its interaction with the rotor dynamic forces, expecting to understand two major observable facts. The first is the prediction of when the pump-turbine will be under RS condition and the second focus on how this RS behavior under determined conditions is, expecting to find appropriate visualization methods to describe and analyze the development and effect of the RS phenomena.

# Notations

---

## Latin

$\tilde{C}_p$	Pressure fluctuation coefficient	[-]
$D$	Reference diameter of the impeller	[m]
$E = gH$	Specific hydraulic energy	[J/kg]
$g$	Gravitational acceleration	[m/s <sup>2</sup> ]
$H$	Hydraulic head	[m]
$k_b$	Number of impeller blades	[-]
$n_{ED}$	Pump-turbine speed factor	[-]
$N_c$	Number of guide vanes	[-]
$Q$	Discharge	[m <sup>3</sup> /s]
$Q_{ED}$	Discharge factor	[-]
$T_m$	Torque	[Nm]
$T_{ED}$	Torque factor	[-]

## Greek

$\alpha_n$	Guide vanes opening	[deg]
$\Gamma$	Coherence	[-]
$\omega_o$	Impeller rotational velocity	[rad/s]
$\rho$	Density of the fluid	[kg/m <sup>3</sup> ]

# Flow Visualization Approach for Periodically Reversed Flows

---

Francisco Botero<sup>1</sup>, Sebastian Guzmán<sup>1</sup>, Vlad Hasmatuchi<sup>2</sup>, Steven Roth<sup>2</sup>, Mohamed Farhat<sup>2</sup>

<sup>1</sup> EAFIT University

Carrera 49 N° 7 Sur - 50, Medellín, Colombia

<sup>2</sup> Laboratory for Hydraulic Machines École Polytechnique Fédérale de Lausanne

Avenue de Cour 33 bis, CH-1007 Lausanne, Switzerland

---

**Abstract:** A non-conventional tufting visualization method along with an image processing development and specific applied technique adapted to the flow conditions is proposed and implemented on a reduced scale model of a Francis-type reversible pump-turbine in three different turbine stages such as turbine mode, runaway mode and turbine break mode, in order to visualize rotating stall phenomenon. Fluorescent monofilament wires along with high speed image processing and pressure sensors were installed in the narrow and vane less gap between the impeller blades and guide vanes. Pressure fluctuations were analyzed along with tuft visualization to describe the flow with and without rotating stall.

**Keywords:** Rotating-Stall, Francis-type pump-turbine, Tuft Visualization.

## 1 Introduction

The flow visualization techniques have been employed in the last 500 years as an experimental study tool of the flow behavior and the phenomena taking place in the interior of the hydraulic machines [1], e.g. turbines, pumps, compressors, to name just a few. Despite it is one of the many available tools in experimental fluid mechanics, is one of the most used because it renders many of the flow field properties directly available to visual perception [2]. Now days a wide variety of techniques to visualize fluid flows are well known and employed in diverse hydraulic machines. Zobeiri [3] performed a velocity survey via Particle Image Velocimetry (PIV) and Laser Doppler Velocimetry (LDV) to study the effect of a hydrofoil trailing edge shape. Sinha et al [4] used PIV to investigate the onset and development of rotating-stall within a centrifugal pump. Navæi [5] developed an experimental Acoustic PIV, measuring the temporal variation in the velocities of particles within some common sound fields. Qian [6] made use of PIV to measure unsteady flows in Francis turbines while Hasmatuchi et al [7] achieved high speed flow visualization with air bubbles injection in a pump turbine under off-design operating conditions.

Although broadly used, these experimental techniques suffer from some problems like affect often the fluid flow, also, not all the flow phenomena or relevant parameters can be visualized with experimental techniques [8]. Furthermore, the construction of small scale physical models and experimental equipment are expensive and the experiments time consuming besides the highly complex instrumentation, also, many of the laser-based techniques, i.e. LDV, PIV are affected by the inherent noise and vibration by the rotational

behavior of the machine, besides the external noise and vibration which often affect experimental results.

In recent years a new research and investigations field has emerged, well-known as Computational Fluid Dynamics (CFD) thanks to the enhance of computational power which has led to an increasing exploit of computers for numerical simulations. In fluid dynamics, computers are broadly employed to calculate velocity fields and other flow quantities using numerical techniques to solve the governing Navier-Stokes equations. This has led into the growth of a relatively new technique known as computer-aided visualization [8]. However, computational studies in hydrodynamic remain limited primarily due to the difficulties in modeling turbulent separated flows in complex geometries that involve interaction between rotating and stationary components [9]. Truthful computational forecast is dependant on user-specified input such as boundary conditions [10], transition and turbulence modeling [11], computational domains that need to be defined for a realistic representation of the specific configuration [12], among others, often depend upon details that often can be obtained only by conducting experiments. Numerical simulations are still under development; approximations of flow patterns despite are sometimes achieved, its results do not fulfill the expectations of fluid engineer community [13]. Reliable visualization of flow phenomena can be based on actual experimental measurements [9], main reason why experimental visualization is still highly employed.

One particular study case in which CFD does not clearly describe the undergoing phenomena is the rotating-stall (RS) [12]. Fringe et al [14] have defined RS as the unsteady flow phenomenon that leads to the incidence of synchronous rotating velocity fluctuations; this is a highly dynamic phenomenon which often occurs in Francis-type reversible pump-turbine. Due to its intrinsic attributes, such as periodicity, flow transition and turbulence, recirculation, stalls, back-flow, swirling flow, among others; the RS is an ideal study case phenomenon which defies the accuracy and adequate evaluation of new flow visualization techniques.

Another visualization technique widely used several years ago is the tuft visualization, commonly used in aerodynamic applications such as wind tunnels [15], compressors [16], among others, frequently employed to study unsteady flow phenomena like RS [17]. Despite this technique has been developed in the aerodynamic field, in hydrodynamic applications is widely utilized in naval researches [18]. Moreover in turbo machinery to study off-design conditions [19] and its associated phenomena for instance RS though it is not clearly detected under certain conditions [20]. Thanks to the recently advances in technology this tuft technique can be proposed as a visualization method along with an image processing development and specific applied technique adapted to the flow conditions that turns this tuft method in a non-conventional tufting visualization.

The accuracy of this novel tuft technique is evaluated under the rotating-stall phenomenon in a Francis-type reversible pump-turbine in generating mode accompanied with pressure sensors carefully installed in the region where the phenomenon manifests. Pressure measurements and other techniques found in the literature for instance Hasmatuchi in [21] were took as reference to validate the results obtained.

## 2 Experimental setup

The flow visualization experimental researches under rotating-stall conditions were accomplished on a reduced scale model of a Francis-type reversible pump-turbine. The center of attention is put on off-design operation regimes: runaway and turbine break modes. Such operation is frequently experienced by pump turbines during the start up process.

A set of 3 test rigs were disposed for testing purposes, performed according to IEC60193 standards [22] within an accuracy of 0.2%. Characteristic curves are traced in terms of the dimensionless factors expressed by equations (1) to (3) describing speed, discharge and torque factor, respectively.

$$n_{ED} = \frac{\omega_o D}{2\pi\sqrt{E}} \quad (1)$$

$$Q_{ED} = \frac{Q}{D^2\sqrt{E}} \quad (2)$$

$$Q_{ED} = \frac{T_m}{\rho D^3 E} \quad (3)$$

Where

Q	is the discharge	[m <sup>3</sup> /s]
T <sub>m</sub>	is the torque	[Nm]
E = gH	is the specific hydraulic energy	[J/kg]
g	is the gravitational acceleration	[m/s <sup>2</sup> ]
H	is the hydraulic head	[m]
ρ	is the density of the fluid	[kg/m <sup>3</sup> ]
ω <sub>o</sub>	is the impeller rotational velocity	[rad/s]
D	is the reference diameter of the impeller	[m]

Technical characteristics of the Francis type reversible pump turbine tested are shown in Table 1.

<i>Parameter</i>	<i>Description</i>	<i>Value</i>
<b><i>k<sub>b</sub></i></b>	Number of impeller blades	9
<b><i>N<sub>c</sub></i></b>	Number of guide vanes	20
<b><i>D<sub>1</sub></i></b>	Impeller inlet diameter	523.5 mm
<b><i>D<sub>1</sub></i></b>	Impeller outlet diameter	250 mm
<b><i>α<sub>n</sub></i></b>	Nominal guide vanes opening	18°

Table 1. Technical parameters of the case study pump-turbine model.

This study case reduced model is a low specific speed pump turbine featuring 9 impeller blades, 20 guide vanes and 20 stay vanes (Figure 1).

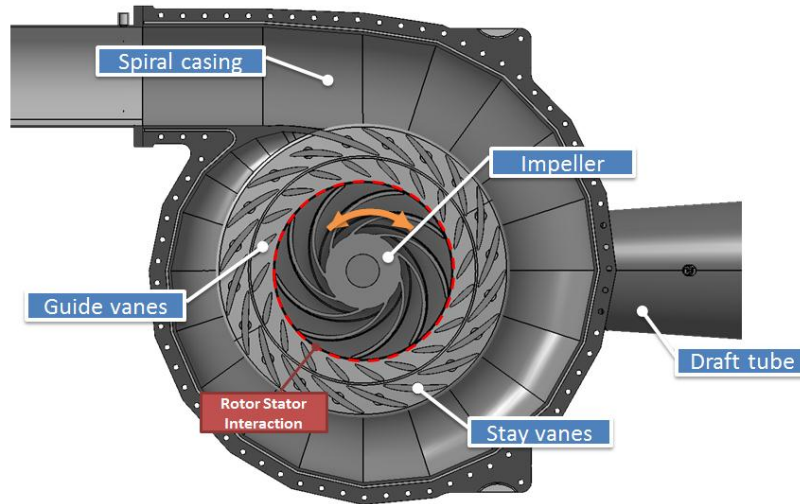


Figure 1. Case study reduced model.

The test head is set to 20m which corresponds to 200 J/Kg specific energy. The guide vanes opening is set to  $\alpha = 10^\circ$  in order to replicate normal startup conditions. Rotational speed is progressively increased from a calm flow operating point to the turbine brake region, via runaway where torque is  $T_{ED} \approx 0$ .

A specific procedure commonly used in model testing of pump turbines[23] is implemented to stabilize the operating point: once at runaway, the butterfly valve located in the main pipe upstream is closed. A by-pass valve equipped with an iris diaphragm is used for fine adjustment of the head valve. Then, the turbine brake mode is explored until a fully developed rotating stall is reached. An unstable characteristics curve is obtained (Figure 2).

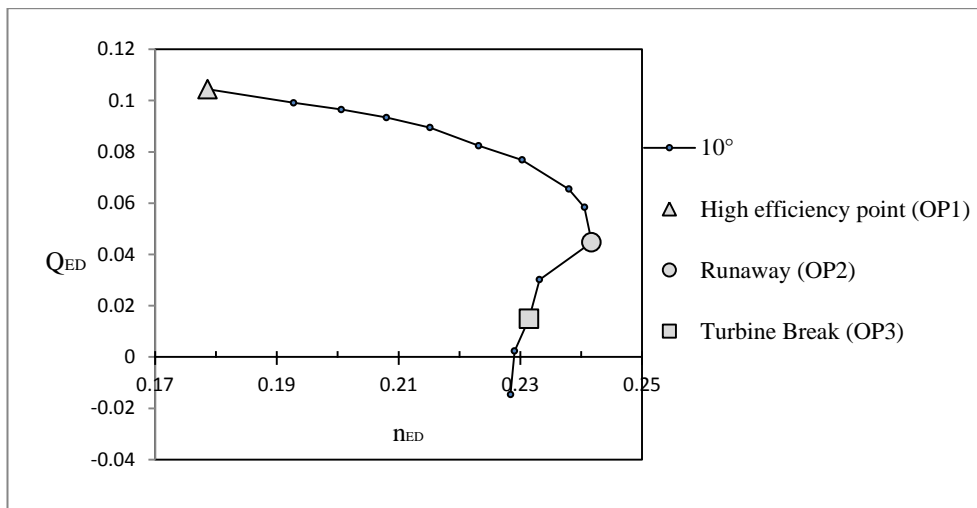


Figure 2.  $Q_{ED}$  curve of the pump-turbine reduced scale model and analyzed operating points.

Different markers are used to indicate the reference operating points (Table 2), OP1 (high efficiency turbine mode), OP2 (runaway mode) and OP3 (turbine break mode)



Point	Description	$Q_{ED}$	$n_{ED}$
OP1	High efficiency point: calm flow	0.0995	0.1933
OP2	Runaway	0.0449	0.2421
OP3	Turbine-brake	0.0148	0.2324

Table 2. Reference points in the turbine.

### 3 Instrumentation

Fluorescent monofilament wires 15mm long and 0.14mm diameter are installed at the upper wall of two consecutive guide vanes, whereas on the midspan of the involved guide vanes (Figure 3).

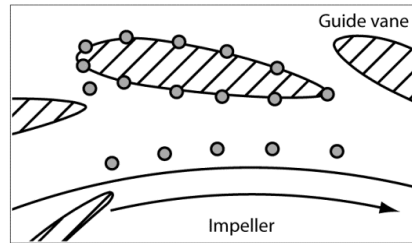


Figure 3. Tufts locations indicated as grey circles

A special technique to attach the wires at the wall surface has been developed by Hasmatuchi in [21]. Holes of 0.5mm diameter and 2mm deep are initially drilled. Anaerobic glue with capillarity properties is injected in the holes with the help of a needle syringe. After, a monofilament wire knotted at one end is introduced into an activator to promote the curing speed of the glue. Finally the attached wires are cut at 15mm length from the wall surface (Figure 4).

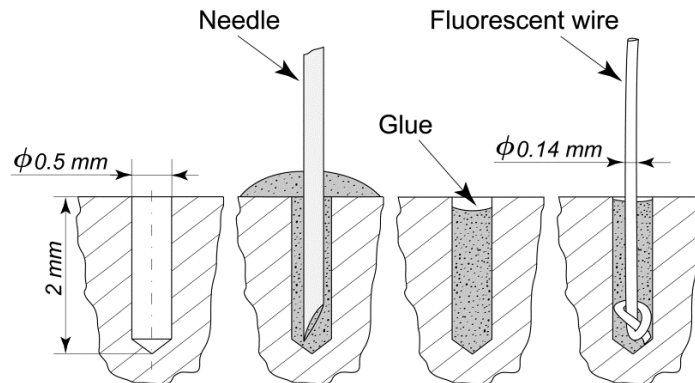


Figure 4. Installation of fluorescent wires for tuft visualization [21].

In no-flow condition the wires are oriented perpendicular to the support surface, while in flow circumstances they are attached to the wall in the direction imposed by the flow. It is assumed that the wires fairly follow the streamlines with no effect on the flow itself [21].

The guide vanes region is observed through a Plexiglass window on the bottom wall of the stator (Figure 5).

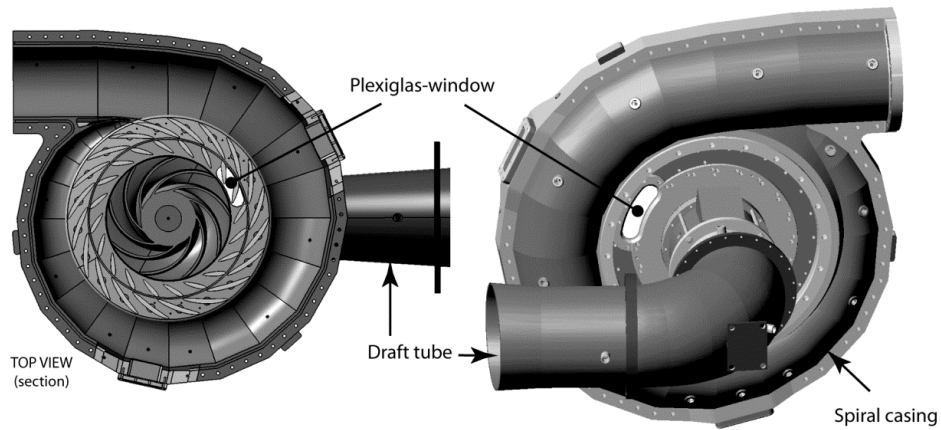


Figure 5. Plexiglas window available in the pump-turbine model, for flow visualization.

To visualize regions of unsteady flow a high speed imaging Photron Fastcam SA1.1 digital camera is used, triggered by the keyphasor and synchronized with pressure measurements. Images of 256x576 pixels are taken at a rate of 10000 fps. Two Cosmobeam 800W sources equipped with linear tungsten halogen bulb provides the lighting of the stage. Ultraviolet components of these bulbs render the fluorescent wires (tufts) visible. Figure 6 shows the experimental setup of the pump-turbine reduced scale model.

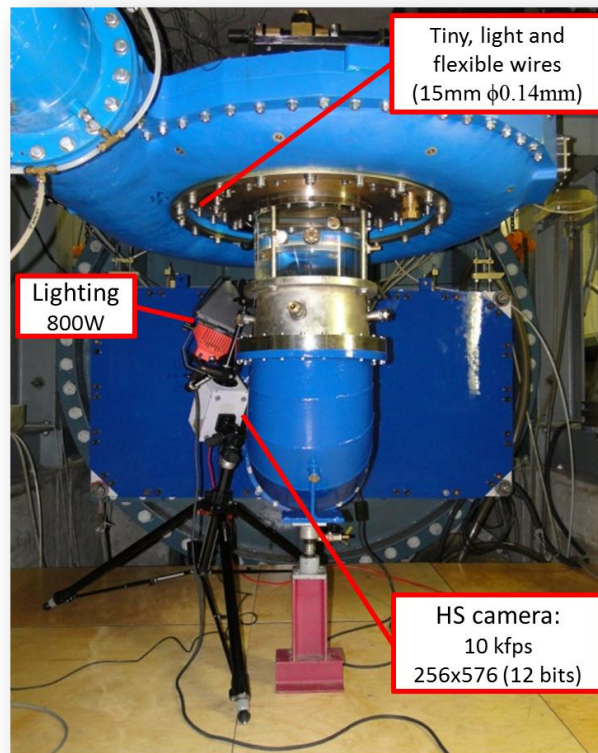


Figure 6. Experimental setup of reduced scale model.

A zero phase reference is resultant from a point on the shaft. An optic sensor observing a rotating hurdle is used to generate a once-per-revolution occurrence. Pressure sensors were

installed in the narrow and vaneless gap between the impeller blades and guide vanes, where the rotor-stator interaction befall.

## 4 Image processing

Unprocessed images hold a lot of information that is not relevant in the case of flow description difficulting the analysis of the movement of the tufts. Therefore an image processing procedure is introduced in order to obtain better analysis results: movie frames were converted to gray scale images. To remove the static objects and get better contrast, consecutive frames are subtracted together. Eventually, the sampling rate is so high or the wires motion so slow that the differences from one frame to the next are negligible, hence, depending on the frame rate, the difference step can be increased to improve the quality of the results.

The projected result is a gray scale image with half of the wires in white and the other half in black, to put them in the same color (white) the absolute value of the resulting frame is calculated, then the color value is inverted in order to have black wires on a white background. This procedure is made for the movie duration so the product is a series of frames that can be superimposed to achieve a final image with the tracks of the wire. A mask containing the guide vane geometry and tuft location is imposed because of the subtraction of all the static objects. Finally, supplementary quality operations may consist in contrast improving, rotation, translation and perspective corrections. Figure 7 summarize the steps followed.

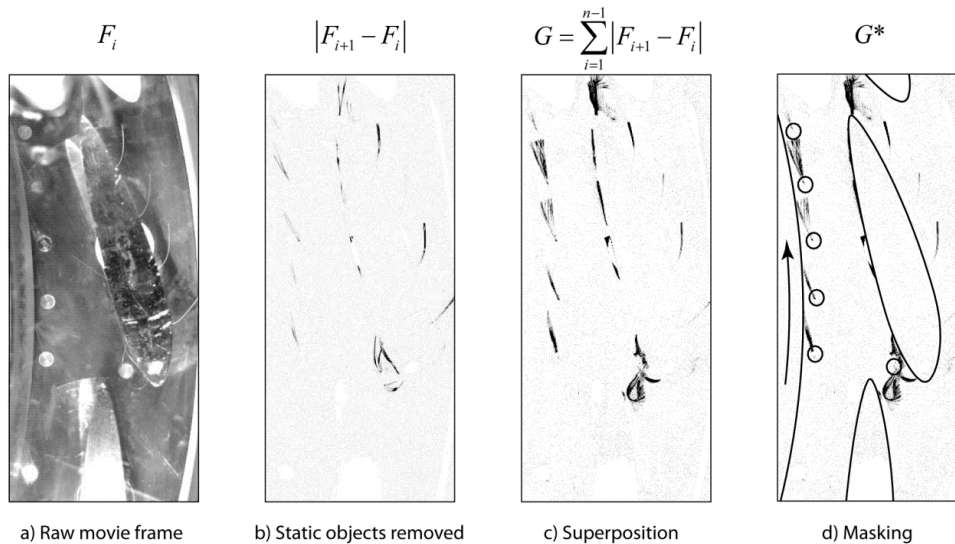


Figure 7. Implemented image processing for tuft visualization. a) Typical frame from high speed movie. b) Consecutive images are subtracted to remove static objects. Moving wires became visible in black by calculating the absolute value. c) The process is repeated for  $n$  images; the  $n-1$  resulting pictures are superposed in order to track the wires positions. d) Guide vanes mask is imposed.

Since impeller rotation and rotation stall are periodic the processing can be synchronized with the phenomenon. It was developed an algorithm presented in equation (4) for the study of the RS phenomenon with the purpose of visualize its propagation around the machine.

Iterative nested cycles cover several RS revolutions and several guide vane channels. At the end, one treated image per guide vane channel is obtained.

$$G_j = \sum_{i=1}^{n-1} |F_{i+1} - F_i|, j = 1, 2, \dots, N_{CH} \quad (4)$$

Where

$F_i$  is the current video frame.

$G_j$  is the processed image for distributor channel  $j$ .

$n = \left\lfloor \frac{N_S}{N_{CH}} \right\rfloor$  is the number of frames per passage of RS by distributor channel.

$N_S$  is the number of frames to complete one revolution of rotating stall.

$N_{CH}$  is the number of channels.

To ensure the Nyquist-Shannon sampling criterion an anti-aliasing low-pass filter is applied to reduce the bandwidth of the movie before it is downsampled.

The cutoff frequency of the filtering process is given by the expression

$$\omega_{max} = \frac{N\omega_{ref}}{2} \quad (5)$$

Where

$\omega_{ref}$  is the angular frequency of the reference tone.

$N$  is the final number of samples per oscillation of the reference tone.

If  $\omega_{ref}$  is replaced by the RS frequency and  $N$  by the number of guide vanes, convenient sequence of averaged image scan be obtained, each one describing the phenomenon in a different guide vanes channel. Assuming  $\omega_{ref} = 0.7\omega_o$  and  $N = 20$ , the cut-off frequency is  $\omega_{max} = 7\omega_o$  it means that the blade passing frequency and following harmonics for the model under test ( $BPF = 9\omega_o$ ) are filtered.

## 5 Results

To describe the flow, along with tuft visualization Pressure fluctuations were analyzed with and without RS. Dimensionless pressure fluctuation coefficient is defined as

$$\tilde{C}_p = \frac{p - \bar{p}}{\rho E} \quad (6)$$

Where

$p$  is the measured pressure [Pa].

$\bar{p}$  is the average pressure [Pa].

$\rho$  is the density of the fluid [ $\text{kg}/\text{m}^3$ ].

$E$  is the specific hydraulic energy [ $\text{J}/\text{kg}$ ].

Video frames and pressure signals are simultaneously recorded and synchronized with the phenomenon. A panoramic representation of RS can be obtained by processing images (one

per guide vane channel) which are prepared in alpha-color layer appended to each image in order to get a transparent background. Then, the tufts are extracted and the resulting reduced image is rotated  $2\pi/N_C = \pi/10$ . Finally, it is translated to the corresponding position according to the polar pattern of the machine geometry. This can be interpreted as RS arrangement.

## 5.1 Rotating stall inception

The machine is driven from a high efficiency and rotating stall free operating point (OP1), to runaway where the rotating-stall beginning is expected. Pressure and processed images at OP1 are shown in Figure 8.

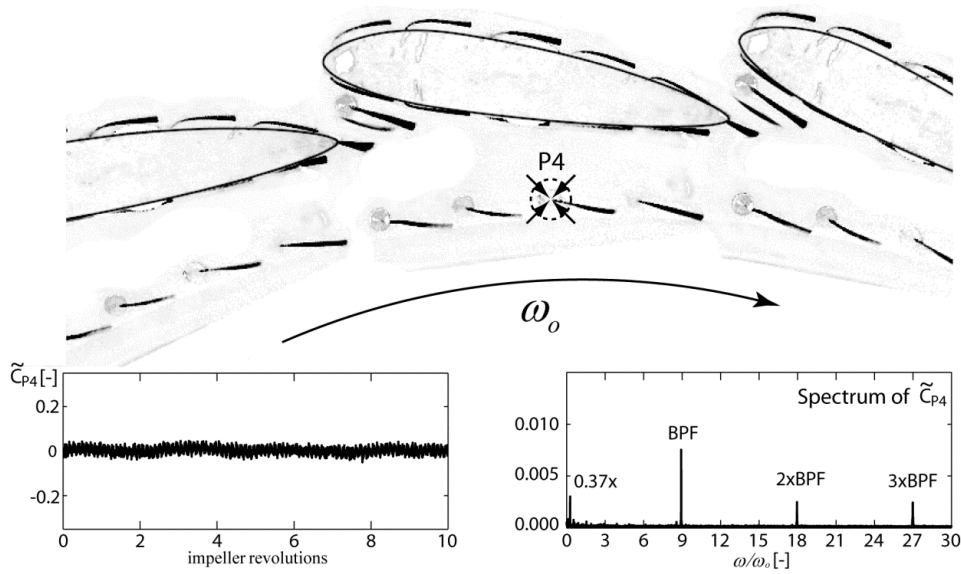


Figure 8.OP1. Tuft visualization and pressure fluctuation over 10 impeller revolutions.

Tufts keep their mean position aligned with the flow with a slight oscillation induced by the impeller blades passage due to a calm flow attached to the hydrofoils. It is complemented by the time and frequency graphics of the pressure coefficient in P4.

Welch's method [24] is employed to estimate the spectrum which is dominated by the impeller blades passing frequency and its harmonics (i.e  $2BPF$  and  $3BPF$ ). A subsynchronous peak at  $0.37\omega_0$  is attributed to a vortex rope in the draft tube, results obtained for turbine mode at OP1 suggests that flow flows relatively orderly revealing pressure fluctuating at the blade passing frequency ( $BPF$ ) along with an unaccented vortex rope.

Flow separation and recirculation is observed when OP2 is reached, causing sporadic blockages into the guide vanes channels (Figure 9). Tufts in the superior plane close to the leading edge shows more activity and most likely flow detachments.

When the tufts located in the vaneless region rest outward, a backflow from the impeller is perceived. Similar strong fluctuations are experienced in the pressure signals whose order is

around ten times stronger than at OP1. In the frequency domain this behaviour is not easily identified; some components take place in the subsynchronous band (from 0 to  $\omega_o$ ) but they are minor compared with the impeller blade passing component.

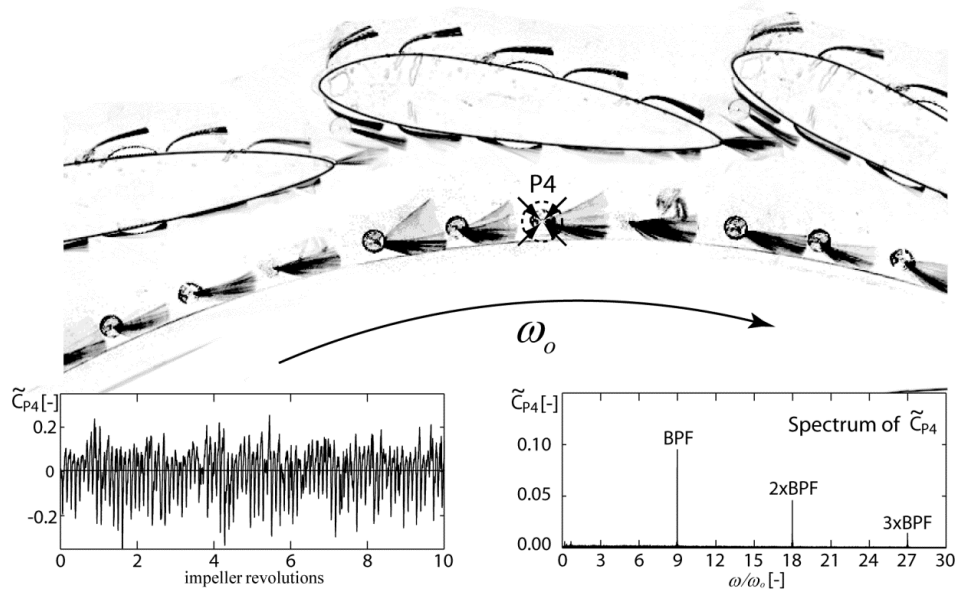


Figure 9. OP2. Tuft visualization and pressure fluctuations in time and frequency domains.

## 5.2 Fully developed rotating-stall

As the machine goes near to the turbine brake mode, flow becomes more disturbed with an increased rotating speed but reduced discharge; this rough flow involving flow separation, vortex formation and back flow among others, converges to a harmonically arranged pattern, the rotating stall is completely developed in OP3. Two different instants, half period apart, are shown in Figure 10 due to the complex flow obtained. The image on the top presents a relative straight flow with the peculiarity that on the bottom side of the guide vanes the fluid seems to flow faster and attached to the surface, however on the opposite side it is not the case.

On the bottom of the Figure 10 a violent stage with strong vortex of straight and reversed flow, detachment and pulsations from the interaction with the impeller blades can be seen. The wires placed between the impeller and the guide vanes or the rotor-stator interaction region presume a confusing evidence because there is not a remarkable difference between them considering both of the images, also, the striking back-flow occurring at OP2 no longer appears at OP3, or at least, not so evidently; this suppose that the average flow all around the vaneless region is the same.

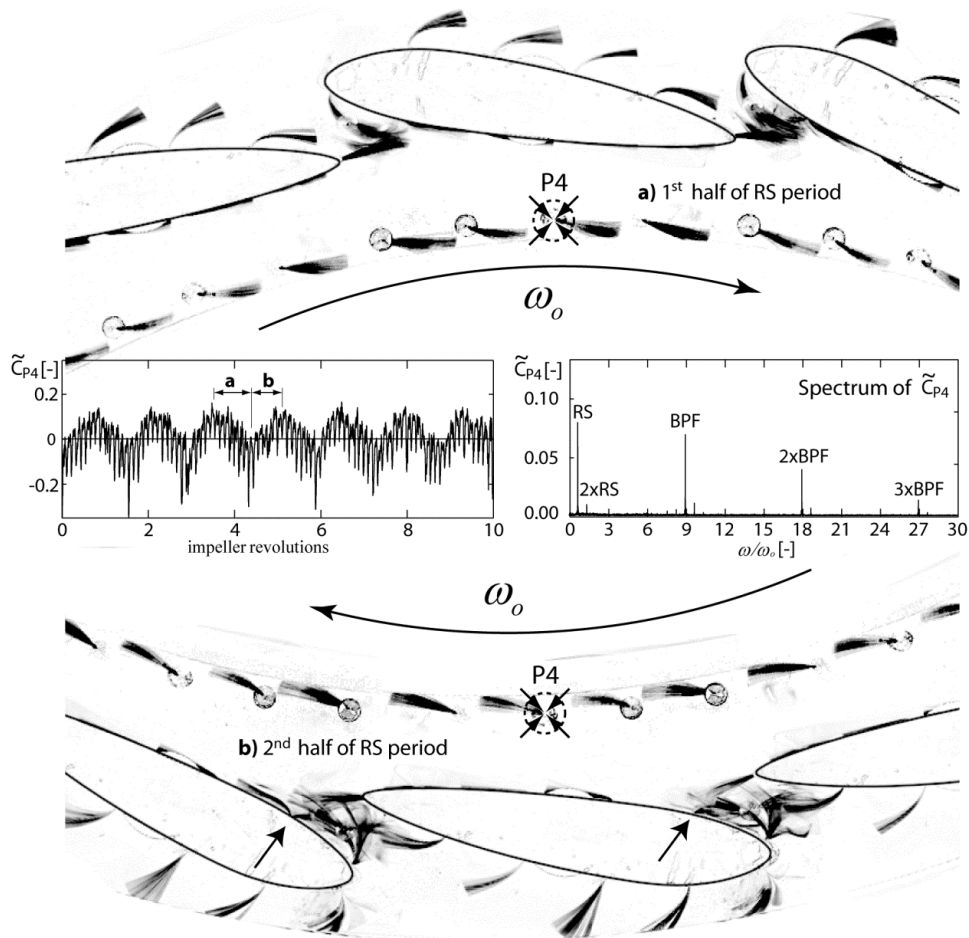


Figure 10.OP3. Tuft visualization and pressure fluctuation from P4, over 10 impeller revolutions. Undergoing rotating-stall becomes evident in time domain as well as in frequency domain. a) Summed images over the 1st half passage of the instability. b) Summed images over the 2nd half of passage of the instability.

The low frequency and quasi-harmonic RS cycle is clearly evident in the pressure coefficient behaviour. Straight flow illustrated on the top image, corresponds to the regions where pressure increases while disturbed flow is experienced during decreasing pressure. The spectrum shows a sharp component arising at  $0.7\omega_o$  as important as the bladed passing pulse, i.e. pressure fluctuations close to 10% of the testing head. A small RS harmonic is also distinguished at  $1.4\omega_o$  and attributed to the shape printed by the passage of the phenomenon: pressure rises rapidly but falls slower.

### 5.3 Negligible Influence of the Tufts

To corroborate the hypothesis of the insignificant influence of the tufts in the flow behaviour, pressure fluctuations are compared in the time and frequency domains with and without tufts at OP1 and OP3. It can be observed in Figure 11 that not only the most prominent components, like RS, BPF and subsequent harmonics are present, but as well no unrelated phenomena can be attributed to the intrusion of the wires proving that, in a macro scale, the flow is not significantly disturbed by the presence of them.

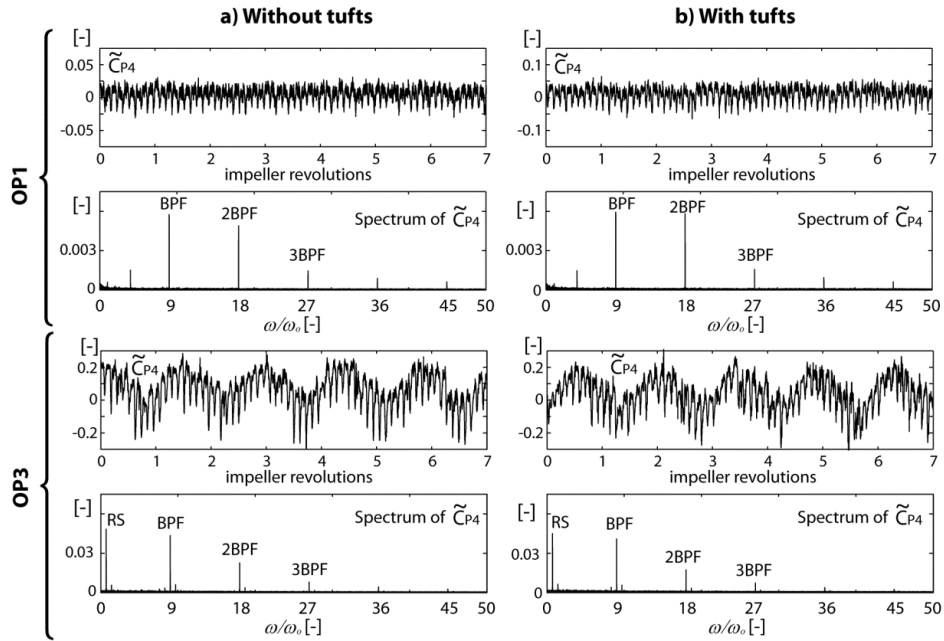


Figure 11. Comparison between pressure fluctuations measured with and without tufts at OP1 and OP3.

## 6 Conclusions

A reduced scale model of a Francis-type pump-turbine was tested under several operating conditions with and without RS. Pressure sensors and tufting with high-speed flow visualization technique was employed to visualize and characterize the RS phenomenon. The implemented tuft visualization method gives an adjusted qualitative description of the undergoing RS phenomena, making evident different flow behaviours such as back-flow, high turbulences, recirculation, among others, attributes that make RS an ideal study case not only in Francis-type pump-turbine but in other turbomachines. The developed visualization method is considered as a non-complicated one, and a feasible experiment technique that can be easily adapted to scientific and industrial communities. By means of specific image processing a panoramic representation of RS was achieved based on the same time-spatial symmetry of the pressure fluctuations. In particular, the RS period is found to consist of four well-define episodes: straight flow with rapidly increasing pressure, flow stagnation, highly disordered flow with decreasing pressure and sudden organization of the flow. The fully developed RS performs at  $0.7\omega_0$  with a single cell. It was recovered from pressure signals and described in by the high-speed tufting visualization.

## 7 Acknowledgments

The present investigation was carried out in the frame work of HYDRODYNA II research project (Eureka N° 4150), in a partnership with ALSTOM Hydro, ANDRITZ Hydro, VOITH Hydro and UPC-CDIF. The authors would like to thank the Swiss Federal Commission for the Technology and Innovation (CTI), Swisselectric Research and Swiss Competence Center of Energy and Mobility (CCEM) for their financial support, as well the HYDRODYNA II partners



for their involvement and support. A special expression of gratitude is conveyed to LMH-EPFL and EAFIT University for their unconditional support.

## 8 References

1. **Cheng, K. C.** A History Of Flow Visualization: Chronology. *Journal of Flow Visualization and Image Processing*. s.l. : Begell House Inc. Publishers, 1997. Vol. 4, 1. ISSN: 1940-4336.
2. **Merzkirch, Wolfgang.** Flow Visualization. s.l. : Academic Press, 2nd Edition, 1987. ISBN: 9780124913516.
3. **Zobeiri, Amirreza.** Effect of Hydrofoil Trailing Edge Geometry on the Wake Dynamics. *PhD Thesis*. Lausanne : École Polytechnique Fédérale de Lausanne, 2012.
4. **Sinha, Manish, Pinarbasi, Ali and Katz, Joseph.** The Flow Structure During Onset and Developed States of Rotating Stall Within a Vaned Diffuser of a Centrifugal Pump. *Journal of Fluids Engineering*. s.l. : ASME, 2001. Vol. 123, pp. 490-499. DOI: 10.1115/1.1374213.
5. **Navæi, Ali Tondast.** Acoustic Particle-Image Velocimetry Development and Applications. *PhD Thesis*. Buckinghamshire : The Open University, 2005.
6. **Qian, Ruixia.** Flow Field Measurements In A Stator Of A Hydraulic Turbine. *PhD Thesis*. Québec : Faculté des études supérieures de l'Université Laval, 2008.
7. **Hasmatuchi, V., et al.** High-speed flow visualization in a pump-turbine under off-design operating conditions. *IOP Conference Series: Earth and Environmental Science*. s.l. : IOP Publishing, 2010. Vol. 12, 1. doi:10.1088/1755-1315/12/1/012059.
8. **Post, Frits H. and van Walsum, Theo.** Fluid Flow Visualization. *Proceedings of Focus on Scientific Visualization*. London, UK : Springer-Verlag, 1993. pp. 1-40. ISBN:3-540-54940-4.
9. **Ullum, Ulrik, et al.** Prediction of rotating stall within an impeller of a centrifugal pump based on spectral analysis of pressure and velocity data. *Journal of Physics: Conference Series* 52. s.l. : Institute of Physics Publishing, 2006. Vols. 36-45. doi:10.1088/1742-6596/52/1/004.
10. **Backman, Alf Gunnar.** CFD Validation of Pressure Fluctuations in a Pump Turbine. *Msc Thesis*. Luleå, Sweden : Luleå University of Technology, 2008. ISSN: 1402-1617.
11. **Sardar, Asad M., et al.** Flow visualization study of an HVAC module operated in water. *2001 Vehicle Thermal Management Systems Conference and Exhibition*. s.l. : Society of Automotive Engineers, Inc, 2001. VTMS-082.
12. **Gourdain, Nicolas, et al.** Simulation of Rotating Stall in a Whole Stage of an Axial Compressor. *Computers & Fluids*. s.l. : Elsevier, 2010. Vol. 39, 9, pp. 1644–1655.
13. **Hasmatuchi, Vlad, et al.** Experimental Evidence of Rotating Stall in a Pump-Turbine at Off-Design Conditions in Generating Mode. *Transactions- American Society of Mechanical Engineers- Journal of Fluids Engineering*. s.l. : American Society of Mechanical Engineers, 2011. Vol. 133, 5. ISSN: 0098-2202.
14. **Fringe, P., and Van Den Braembussche, R.** Distinction Between Different Types of Impeller and Diffuser Rotating Stall in a Centrifugal Compressor with Vaneless Diffuser. *Journal of Engineering for Gas Turbines and Power, Transactions*. s.l. : American Society of Mechanical Engineerings, 1984. Vol. 106, 2, pp. 468-474.

15. **Ristić, Slavica.** Flow Visualisation Techniques in Wind Tunnels Part I – Non optical Methods. *Scientific Technical Review*. 2007. Vol. 62, 1, pp. 39-50.
16. **Myose, Roy Y., Hayashibara, Shigeo and Heron, Ismael.** Flow Visualization Study on the Effect of a Gurney Flap in a Low Reynolds Number Compressor Cascade. *6th AIAA Aviation Technology, Integration and Operations Conference (ATIO)*. Wichita : American Institute of Aeronautics and Astronautics Inc, 2006.
17. **Thiam, Aicha H, et al.** Corner Separation and the onset of stall in an axial compressor. *American Physical Society, 60th Annual Meeting of the Division of Fluid Dynamics*. s.l. : American Institute of Aeronautics and Astronautics Inc, 2008.
18. **Denz, Thomas, Smith, Stephanie and Shrestha, Rajeev.** Multi-hull Flow Visualization: An investigation of flow visualization techniques for trimaran hulls. *Final rept. 21 May-10 Aug 2007*. West Bethesda, MD : Naval Surface Warfare Center Carderock Div., 2007.
19. **Bhattacharyya, Abhijit, et al.** Observations On Off-Design Flows In Non-Cavitating Axial Flow Inducers. *ASME Symposium on Pumping Machinery. Fluids Engineering Division, FED-154 (154)*. New York : American Society of Mechanical Engineers, 1993. pp. 135-141.
20. **Yadoiwa, A., et al.** rotating stall in mixed-flow turbomachines. *Twelfth Australasian Fluid Mechanics Conference*. Sydney : The University of Sydney, 1995. pp. 69-72.
21. **Hasmatuchi, Vlad.** Hydrodynamics of a Pump-Turbine Operating at Off-Design Conditions in Generating Mode. *PhD Thesis*. s.l. : École Polytechnique Fédérale de Lausanne, 2012.
22. **International Electrotechnical Committee .** Hydraulic Turbines, Storage Pumps and Pump-Turbines – Model Acceptance Tests. *International Standard IEC 60193*. 2006. BS EN 60193:1999.
23. **Dörfler, P.K, et al.** Stable Operation Achieved on a Single-Stage Reversible Pump-Turbine Showing Instability at No-Load. *Proceedings of the 19th IAHR Symposium on Hydraulic Machinery and Cavitation, Singapore*. 1998. pp. 431-440.
24. **Welch, Peter D.** The use of fast fourier transform for the estimation of power spectra: A method based on time averaging over short, modified periodograms. *IEEE Transactions on Audio Electroacoustics*. 1967. Vols. AU-15, 70–73.

# Experimental Rotordynamics of a Francis-Type Pump-Turbine in Generating Mode at Off-Design Operating Conditions

---

Sebastian Guzmán<sup>1</sup>, Francisco Botero<sup>1</sup>, Vlad Hasmatuchi<sup>2</sup>, Steven Roth<sup>2</sup>, Mohamed Farhat<sup>2</sup>

<sup>1</sup> EAFIT University

Carrera 49 N° 7 Sur - 50, Medellín, Colombia

<sup>2</sup> Laboratory for Hydraulic Machines École Polytechnique Fédérale de Lausanne

Avenue de Cour 33 bis, CH-1007 Lausanne, Switzerland

---

**Abstract:** A reduced scale models of a Francis-type reversible pump-turbine in generating mode was investigated in three different stages such as turbine mode, runaway mode and turbine break mode, in order to identify and detect rotating stall phenomenon from rotordynamics standpoint. Two proximity probes were orthogonally embedded into the main bearing along with a keyphasor allowing positive results detecting the rotating stall in the particular analyzed case. Pressure measurements were analyzed along with proximity probes to correlate the shaft precession with the induced sub-synchronous flow instability.

**Keywords:** Rotating-Stall, Francis-type pump-turbine, Rotordynamics in turbine.

## 1 Introduction

Pump turbines technology is widely seen as having a great potential in storing large amounts of electrical energy [1]. This kind of turbo machinery provides a way in which control power grid because gives an efficient manner to stabilize the electricity by moving water forth and back between upstream and downstream reservoirs to attain both the energy supply and demand [2]; it combines both axial and radial flow concepts to take energy from or to add energy to a fluid, therefore, is subjected to frequent switching between pumping and turbine modes with extensive periods under off-design conditions. Five main operating regimes can be distinguished: pump mode, pump brake, turbine mode, turbine break and reverse pump; a deeper description of the phenomena involved of each region mode can be found in Amblard et al. [3]. Due to this different regimes, during the operation at any operating point, the relative motion between the impeller blades and guide vanes induces pressure fluctuations that propagate through the entire machine [4] giving raise to severe oscillations at off-design conditions [5], further under specific conditions, a stationary separation zone may begin to progress known as rotating-stall (RS).

The RS is a hydrodynamic phenomenon occurring in Francis-type reversible pump-turbines for example when the machine is required to run at low guide vanes opening. Fringe et al. [6] defined it as an unsteady flow phenomenon that leads to the incidence of synchronous rotating velocity fluctuations; the stall is a highly dynamic phenomenon which can take place in impellers and/or stationary components of hydraulic machines [7], this causes a small

region of lower speed flow through the machine around the machine with a sub-synchronous precession with rotative speed dependant frequency at a speed lower than the rotor speed [8].

The interest in radial flow instabilities, such as this sub-synchronous phenomenon has been widely studied, found to be in general at 0.10x-0.20x rotating speed when action occurs in the diffuser and at 0.60x-0.80x rotating speed when action takes place in the impeller [9] also simulations of RS cell propagation [10] as well as control stabilization of flow at the inception of RS [11] have been developed. Furthermore, diverse techniques have been employed in RS detection, Yadoiwa et al. [12] used flow visualization tufts to study RS at impeller inlet while Shina et al. [13] employed particle image velocimetry (PIV) and pressure fluctuation measurements for investigate the onset and development of RS inside a centrifugal pump. Nonetheless, approximations of flow patterns surrounded by RS have been achieved with the development of numerical simulations [14], although, the obtained results are not entirely accepted among the fluid engineering community [15]; besides, the understanding of the steady and unsteady forces and the related rotordynamic behavior is requisite to model turbo machines effectively [16].

Even though, the broadly employment of diverse techniques, the advances in understanding of rotordynamics through the non contact probes for observing shaft motion directly [17] has evolved into the study of rotordynamic forces in turbo machinery. Bentley et al. [18] and [19] discuss RS in centrifugal compressors from vibration diagnostics and rotordynamics stand points concluding that during RS the rotordynamic stability margin is reduced and usually results in the appearance of a low sub-synchronous rotor vibration level caused by a RS at the design stage of centrifugal compressor. Also, they conclude that the emphasis on rotor behavior does not allow for details of particular flow patterns, but treats the fluid "in average" which falls in the scale of rotor motion. Despite this, the literature survey shows insufficient understanding of rotordynamic implications of RS, especially in Francis-type reversible pump-turbines were no publications are found; being that scope of this work.

## 2 Experimental Setup

The experimental investigations for the detection of rotating stall were accomplished on a reduced scale model of a Francis type reversible pump turbine. The center of attention is put on off-design operation regimes: runaway and turbine break modes. Such operation is frequently experienced by pump turbines during the start up process.

A set of 3 test rigs (Figure 1) were disposed for testing purposes, performed according to IEC60193 standards [20] within an efficiency accuracy of 0.2%.

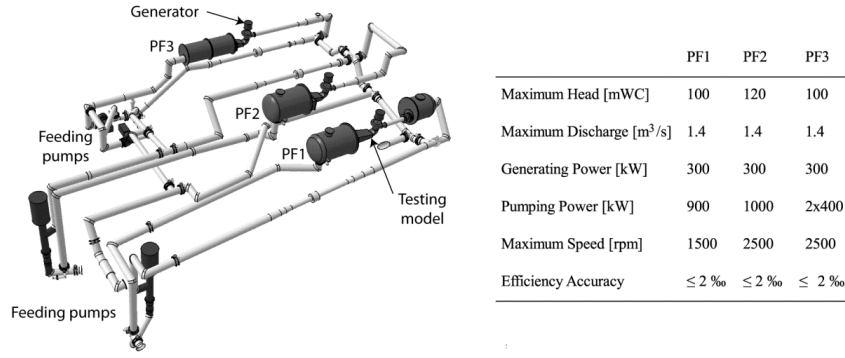


Figure 1. EPFL-LMH experimental test rigs (courtesy: EPFL-LMH, 2011)

Technical characteristics of the Francis type reversible pump turbine tested are shown in Table 1.

Parameter	Description	Value
$k_b$	Number of impeller blade	9
$N_c$	Number of guide vanes	20
$D_1$	Impeller inlet diameter	523.5 mm
$D_1$	Impeller outlet diameter	250 mm
$\alpha_n$	Nominal guide vanes opening	18°

Table 1. Technical parameters of the case study pump-turbine model

Characteristic curves in function of discharge  $Q$ , torque  $T_m$ , specific hydraulic energy  $E = gH$ , gravitational acceleration  $g$ , hydraulic head  $H$ , density  $\rho$ , impeller rotational velocity  $\omega_o$  and reference diameter of the impeller  $D$  are traced in terms of the dimensionless factors expressed by equations (1) to (3) describing speed, discharge and torque factor, respectively.

$$n_{ED} = \frac{\omega_o D}{2\pi\sqrt{E}} \quad (1)$$

$$Q_{ED} = \frac{Q}{D^2\sqrt{E}} \quad (2)$$

$$Q_{ED} = \frac{T_m}{\rho D^3 E} \quad (3)$$

This study case reduced model is a low specific speed pump turbine featuring 9 impeller blades, 20 guide vanes and 20 stay vanes (Figure 2).

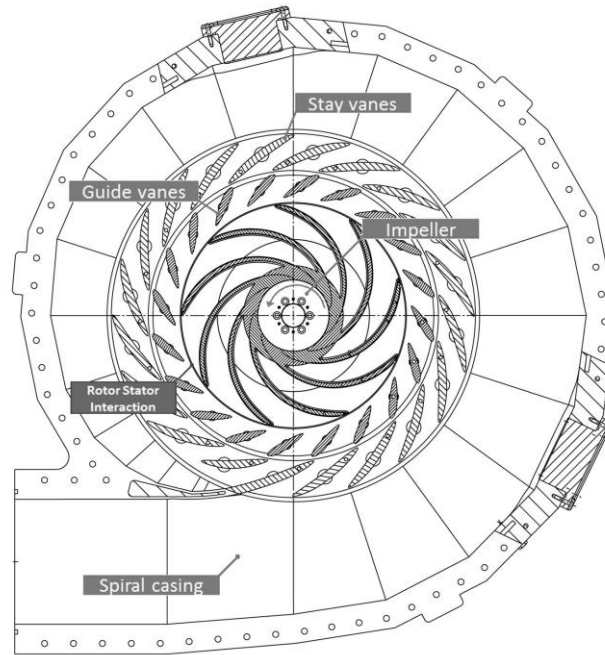


Figure 2. Case study reduced model.

The test head is set to 20m which corresponds to 200 J/Kg specific energy. The guide vanes opening are set to  $\alpha = 10^\circ$  in order to replicate normal startup conditions. Rotational speed is progressively increased from a calm flow operating point to the turbine brake region, through runaway where torque is  $T_{ED} \approx 0$ .

A specific procedure commonly used in model testing of pump turbines [21] is implemented to stabilize the operating point: once at runaway, the butterfly valve located in the main pipe upstream is closed. A by-pass valve equipped with an iris diaphragm is used for fine adjustment of the head valve. Then, the turbine brake mode is explored until a fully developed rotating stall is reached. An unstable characteristics curve is obtained (Figure 3).

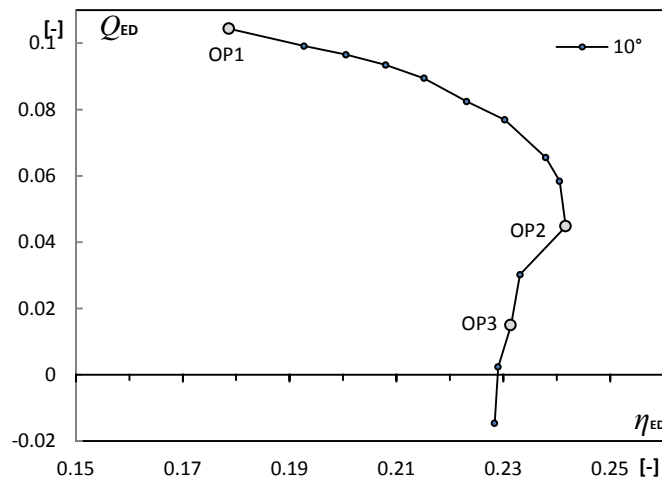


Figure 3.  $Q_{ED}$  Curve of the pump-turbine reduced scale model and analyzed operating points.

Pressure sensors were installed in the narrow and vaneless gap between the impeller blades and guide vanes, where the rotor-stator interaction befall. A zero phase reference (known as keyphasor) is resultant from a point on the shaft. An optic sensor observing a rotating hurdle is used to generate a once-per-revolution occurrence.

Two non-contact, eddy-current proximity probes are used to reconstruct shaft orbits; both of the proximity probes are orthogonally arranged in order to allow a simple reconstruction of the shaft orbits, mounted in the bearing housing of the main journal bearing (Figure 4).

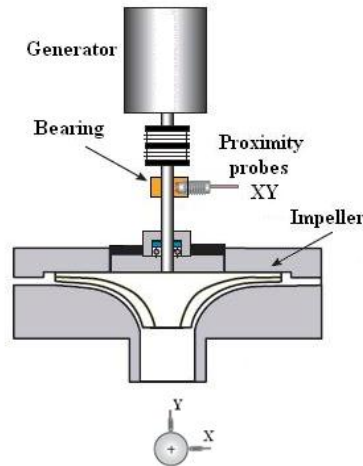


Figure 4. Experimental setup

Berten in [7] showed that, for centrifugal pumps, the shaft position is affected by the balance between the mechanical and hydraulic forces wield on the impeller, thus any variation in such forces results in a displacement of the shaft.

### 3 Results

Proximity probes orthogonally implanted in the main bearing are employed to obtain the movement of the shaft during operation. The shaft position is influenced by the disequilibrium between the mechanical and hydraulic forces wield on the impeller, variation in such forces provoked by an undergoing RS outcome in the displacement of the shaft.

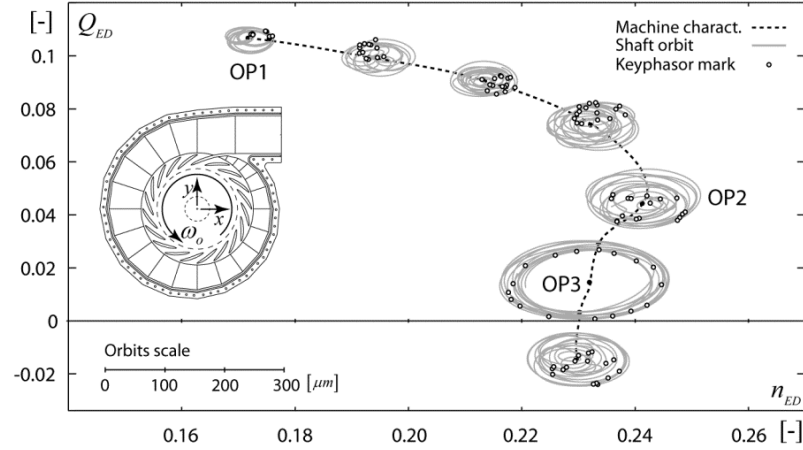


Figure 5. Shaft Orbits and S-shaped characteristics. The orbit plot shows the dynamic motion of the centre of the rotating impeller with signals from proximity probes X and Y.

Samples are taken at different operating points, from OP1 and going up to the reverse pump mode. Figure 5 shows an overview of the rotordynamics for positive rotation quadrants. Scaled versions of the orbits and the respective keyphasor marks (pulse per revolution) are depicted on the performance characteristics. For each operating point, an orbit is a two-dimensional image of the shaft center motion. Proximity signals are lowpass filtered in order to preserve the subsynchronous band ( $\omega/\omega_o \leq 1$ ), the region of where RS manifest.

The orbital motion around OP1 exhibit lateral synchronous vibrations with small amplitudes caused by the inertia forces of a residual unbalance of the rotor. These vibrations are stable at constant rotation speeds since the keyphasor marks remains always on the same quadrant while at runaway (OP2) and reverse pump mode; the orbit pattern is no longer followed, revolutions rather seems to start and finish on random positions. On the other hand, just between runaway and reverse pump during turbine brake rotation (OP3), an outstanding new pattern is generated: concentric elliptical orbits featuring marks equally distributed around them. In Figure 6 operating points OP1, OP2 and OP3 can be analyzed independently.



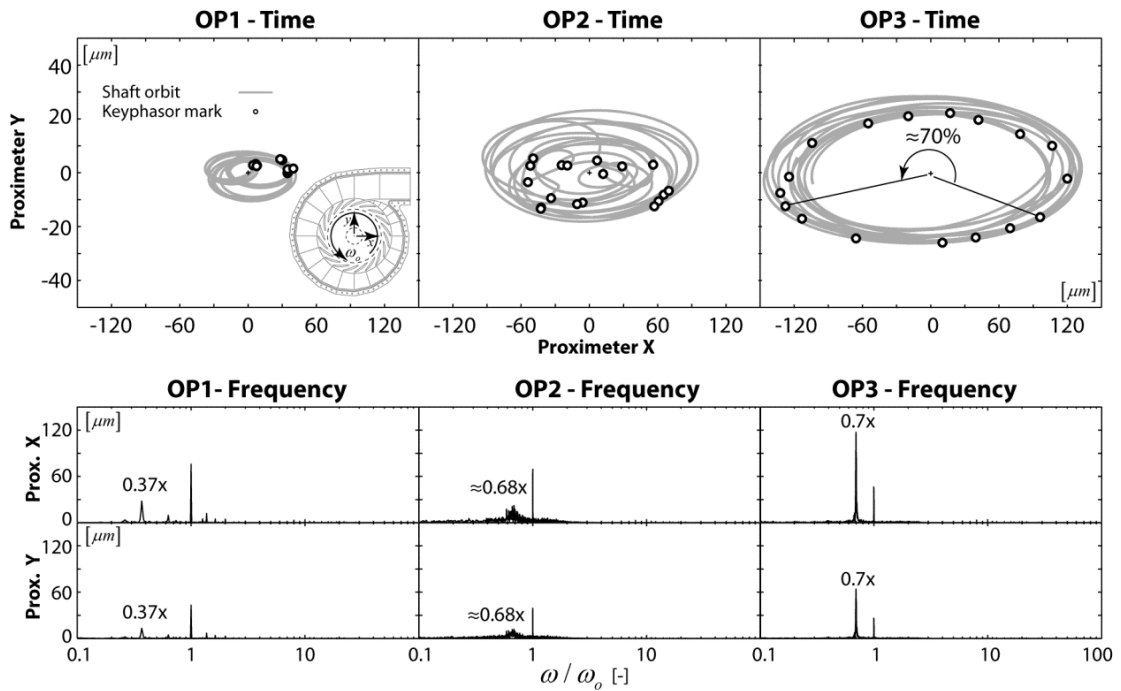


Figure 6. Shaft precession for OP1, OP2 and OP3, during few revolutions.

Spectral estimations are given for both of the proximity signals used to build the orbits. Synchronous lateral vibrations are always observed. The component rising at  $0.37x$  is related to a vortex rope developed in the draft tube at OP1. Likewise, at OP2 the energy concentrated around  $0.68x$  is attributed to the onset of RS which becomes sharper and dominant at OP3. At that point, consecutive keyphasor marks are separated by an angle of about  $252^\circ$ , i.e. 70%.

### 3.1 OP1

Besides the observed synchronous vibration, a minor radial unbalanced load on the rotor produces a low frequency oscillation attributed to a vortex rope evolving in the draft tube. The coherence of the signal from one pressure sensor placed on the draft tube together with the signal obtained from the proximity probes is plotted in Figure 7 using logarithmic frequency scale; the high coherence around  $0.37\omega_0$  implies that the origin of the perturbation is noticeably found in the draft tube, where the pressure monitoring point is located.

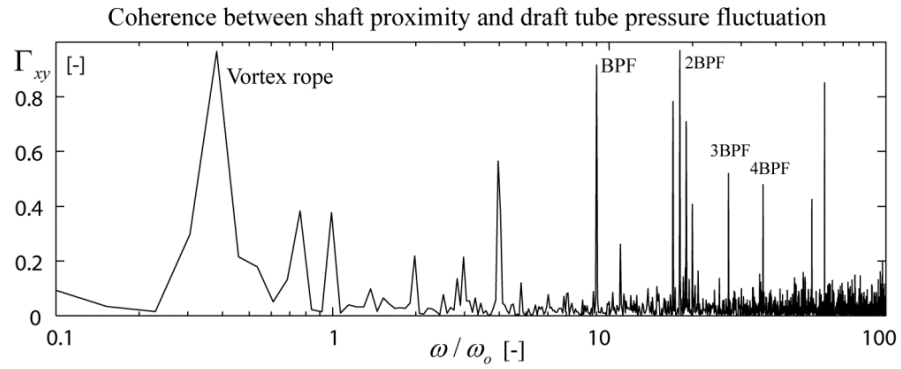


Figure 7. Vortex Rope. Coherence estimated between signals from the proximity probe x and the pressure monitoring point located in the draft tube.

### 3.2 OP2 (Runaway)

A less stable behaviour than OP1 is observed due to the amplitude of the shaft orbits, which despite of being concentric, its shape begins to distort as well as the location of the keyphasor marks. Sudden changes and small loops can be seen as shaft's reaction to sporadic blockages because of the RS inception that appears in guide vanes or impeller channels.

The uneven flow developed can create numerous kinds of hydrodynamic instabilities as local vortices or eventual stalls that may or not rotate. This subsynchronous perturbation is rather linked to hydrodynamic events, but to differentiate it from other perturbation sources like mechanical faults, proximity signals are compared together with the pressure signals taken from the distributor channels employing coherence function (Figure 8).

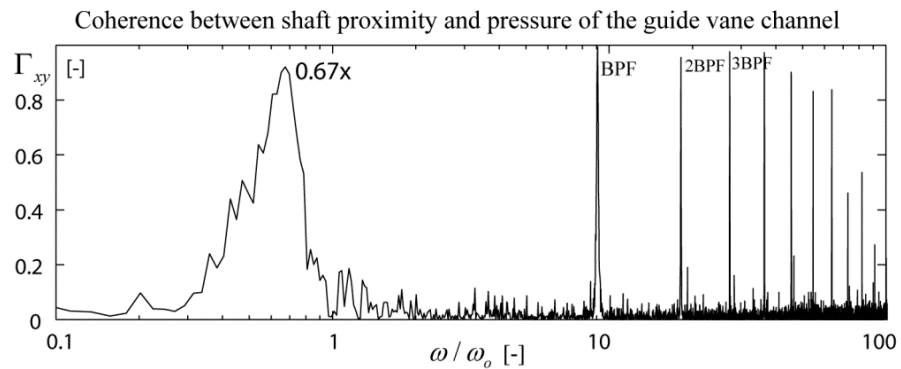


Figure 8. RS inception. Coherence estimated between signals from the proximity probe x and the pressure monitoring point P4, located in the vaneless gap between the impeller and guide vanes.

### 3.3 OP3 (fully developed RS)

At OP3 the undergoing RS gets fully developed, its existence oblige the orbits to be concentric again but exposing a different pattern featuring a new aspect of the order lost at OP2: The amplitudes of the described orbits are homogeneous and their phases, followed by the keyphasor marks are 252° distant.

It can be said that irregularly distributed pressure around the impeller produces an intense unbalance perceived by the shaft and altering its precession; the system behaves like a rotating cantilever beam, which explains the resulting orbits as can be seen in Figure 9.

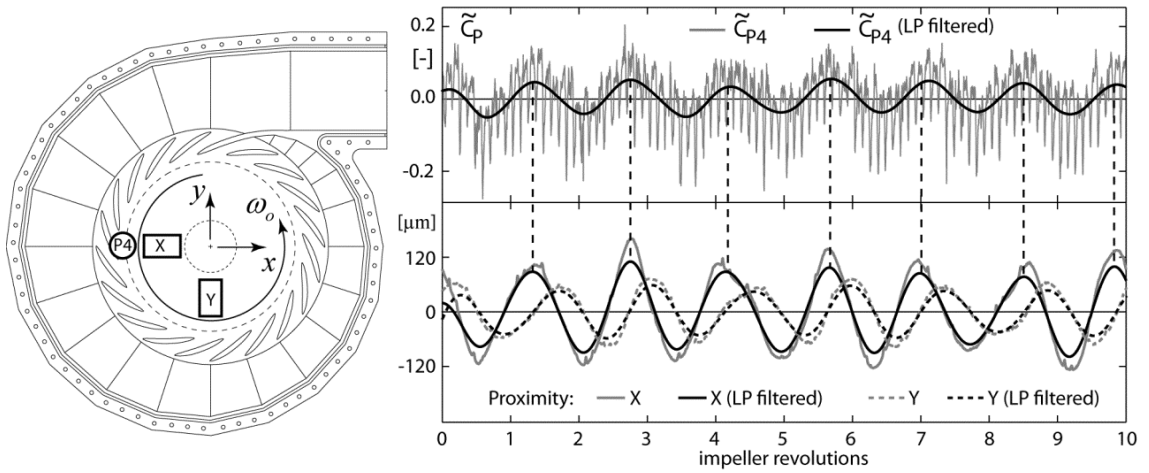


Figure 9. Pressure fluctuation and shaft motion.

Synchronized signals from pressure sensor P4 and proximity probes X and Y are used to show the coherence of the RS related pressure and shaft eccentricity. Low pass (LP) filtered signals are also included to facilitate understanding. Vertical dashed lines indicates synchronization between P4 and X; i.e. the higher the pressure, the further the center of the shaft.

## 4 Discussion

The coherence between the hydrodynamic parameters such as pressure measurements and the signals of the mechanical parameters such as proximity probes shows that frequency component described by the precession of the shaft is highly coherent with the observed pressure fluctuations, thus it indicates that the precession of the shaft is due to the undergoing RS rather than unrelated mechanical behaviors. For the obtained pattern, both the orbits and the spectrum, evidence the manifestation of the studied phenomenon especially notorious in OP3 in which the component rising at  $0.7x$  is linked with RS that becomes sharper, dominant and where consecutive keyphasor marks are equally separated.

Nonetheless, other phenomena of different nature (mechanical, for instances) might show similar behavior, particularly in the case of shafts supported by journal bearings. In some cases, highly dynamic phenomena are induced by interaction between the rotor and bearing or seal fluid motion. For example oil-whip described in Muszynska in [22] appears to have similar signatures and orbits. Even though, this method seems to be assertive enough since the similarity of the orbits is far enough in frequency spectrum to differentiate between mechanical and hydrodynamic phenomena in view of the fact that oil-whip most likely produce vibration instabilities at  $0.47x$  [23], that is, a difference of about 30% of the

subsynchronous frequency. Therefore diagnose this kind of hydraulic phenomena based on mechanical elements is plausible and accurate without the interference of any additional mechanical phenomena for the study case developed.

As these sensors are already installed in most turbo machinery since several years ago, this method could become a practical low-cost solution and almost implementation-free for the detection of RS. However, one specific case where this method might not work is when RS develops in more than one cell symmetrically because they tend to redistribute the pressure around the axis as reported by Braun in [24], causing the system to equilibrate making detection procedures more complicated. In that case, the low frequency can be still detectable, but the number of cells, probably not; in contrast with the occasion of a single cell or non-symmetrical arrangements which yields to a high and a low pressure zones around the impeller usually half circumference apart, whose generate significant unbalance affecting the precession of the shaft. Even so, according to literature Francis-type pump-turbines in generating mode, the RS is prone to occur in one single cell, different to the pump mode, where this phenomenon may be deeper explored.

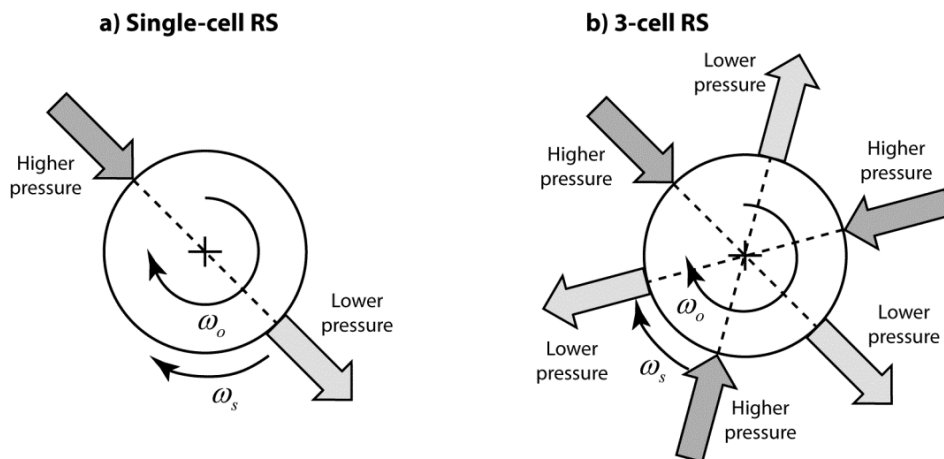


Figure 10. Expected shaft loads caused by pressure distribution around the impeller in the case of: a) single-cell RS, or b) 3-cells RS.

## 5 Conclusions

Two proximity probes were orthogonally embedded into the main bearing along with a keyphasor allowing positive results detecting the rotating stall in the particular analyzed case. The diagnose of this kind of hydraulic phenomena based on mechanical elements is plausible and accurate by means of this method besides other phenomena might show similar behavior and eventually confound the analysis under certain conditions. Anyhow, as the RS generally outcomes in the manifestation of a low sub-synchronous frequency component in the rotor spectrum, near operating conditions the frequencies due to the hydraulic phenomena such as RS have shown to be far enough from frequencies of mechanical phenomena for instance, oil-whip, allowing an accurate diagnosis.

However, if RS develops in more than one cell symmetrically, the expected distribution of the pressure tends to equilibrate the hydrodynamic loads in the impeller and therefore in the shaft. The present characteristic pattern revealing a strong unbalance is no longer respected making the detection complicated. Even so, in Francis-type pump-turbines in generating mode the RS is susceptible to occur in one single cell.

## 6 Acknowledgments

The present investigation was carried out in the frame work of HYDRODYNA II research project (Eureka N° 4150), in a partnership with ALSTOM Hydro, ANDRITZ Hydro, VOITH Hydro and UPC-CDIF. The authors would like to thank the Swiss Federal Commission for the Technology and Innovation (CTI), SWS Electric Research and Swiss Competence Center of Energy and Mobility (CCEM) for their financial support, as well the HYDRODYNA II partners for their involvement and support. A special expression of gratitude is conveyed to LMH-EPFL and EAFIT University for their unconditional support.

## 7 References

1. **Hasmatuchi, Vlad, Farhat, Mohamed and Avellan, François.** Hydrodynamics of a Pump-Turbine under Off-Design Operating Conditions in Generating Mode. *Proceedings of the 1st EPFL Doctoral Conference in Mechanics*. Lausanne : EPFL Doctoral Conference in Mechanics - EDCM2010, 2010. págs. p. 111-114.
2. **Hasmatuchi, V., et al.** High-speed flow visualization in a pump-turbine under off-design operating conditions. *IOP Conference Series: Earth and Environmental Science*. s.l. : IOP Publishing, 2010. Vol. 12, 1. doi:10.1088/1755-1315/12/1/012059.
3. **Amblard, H, et al.** Behavior of Francis Turbines and Pump-Turbines at Partial Flow. *La Houille Blanche*. 1985. 5, págs. 435-440. DOI: 10.1051/lhb/1985031.
4. **Zobeiri, Amirreza.** Effect of Hydrofoil Trailing Edge Geometry on the Wake Dynamics. *PhD Thesis*. Lausanne : École Polytechnique Fédérale de Lausanne, 2012.
5. **Drtna, P and Sallaberger, M.** Hydraulic turbines—basic principles and state-of-the-art computational fluid dynamics applications. *Proceedings of the Institution of Mechanical Engineers, Part C: Journal of Mechanical Engineering Science*. 1999. Vol. 213, 1, págs. 85-102. doi: 10.1243/0954406991522202.
6. **Fringe, P and Van Den Braembussche, R.** Distinction Between Different Types of Impeller and Diffuser Rotating Stall in a Centrifugal Compressor with Vaneless Diffuser. *Journal of Engineering for Gas Turbines and Power, Transactions*. s.l. : American Society of Mechanical Engineerings, 1984. Vol. 106, 2, págs. 468-474.
7. **Berten, S.** Hydrodynamics of High Specific Power Pumps for Off-Design Operating Conditions. *PhD Thesis*. Lausanne, Switzerland : EPFL, 2010.

8. **Thiam, Aicha H, et al.** Corner Separation and the onset of stall in an axial compressor. *American Physical Society, 60th Annual Meeting of the Division of Fluid Dynamics*. s.l. : American Institute of Aeronautics and Astronautics Inc, 2008.
9. **Teeling, Sebastiaan.** Using data manager 2000 to remotely diagnose gas compressor rotating stall. *Orbit*. 1998. Vol. 19, 4, págs. 26-29.
10. **Lewis, Ivan R.** Study of blade to blade flows and circumferential stall propagation in radial diffusers and radial fans by vortex cloud analysis. *Journal of Computational and Applied Mechanics*. 2004. Vol. 5, 2, págs. 323-335.
11. **Belta, Calin, et al.** Rotating stall control for axial flow compressors. *Automatica*. s.l. : Elsevier Science Ltd, 2001. Vol. 37, págs. 921-931.
12. **Yadoiwa, A., et al.** rotating stall in mixed-flow turbomachines. *Twelfth Australasian Fluid Mechanics Conference*. Sydney : The University of Sydney, 1995. págs. 69-72.
13. **Sinha, Manish, Pinarbasi, Ali and Katz, Joseph.** The Flow Structure During Onset and Developed States of Rotating Stall Within a Vaned Diffuser of a Centrifugal Pump. *Journal of Fluids Engineering*. s.l. : ASME, 2001. Vol. 123, págs. 490-499. DOI: 10.1115/1.1374213.
14. **Gourdain, Nicolas, et al.** Simulation of Rotating Stall in a Whole Stage of an Axial Compressor. *Computers & Fluids*. s.l. : Elsevier, 2010. Vol. 39, 9, págs. 1644-1655.
15. **Hasmatuchi, Vlad, et al.** Experimental Evidence of Rotating Stall in a Pump-Turbine at Off-Design conditions in Generating Mode. *Journal of Fluids Engineering, Transactions of the ASME*. s.l. : American Society of Mechanical Engineers, 2011. Vol. 135, 5. ISSN: 0098-2202.
16. **Guinzburg, A, et al.** Rotordynamic forces generated by discharge-to-suction leakage flows in centrifugal pumps. *Proceedings 1990 conference on advance Earth-to-Orbit propulsion technology*. Huntsville, Alabama : NASA, 1990.
17. **Gunter, Edgar J.** Understanding amplitude and phase in rotating machinery. *Vibration institute 33rd annual meeting*. Harrisburg, Pa : s.n., 2009.
18. **Bently, Donald E., Goldman, Paul and Yuan, Jing.** Rotor Dynamics of Centrifugal Compressors in Rotating Stall. *Orbit*. 2001. Vol. 22, págs. 40-50.
19. **Bently, Donald E. and Goldman, Paul.** Vibrational Diagnostics of Rotating Stall in Centrifugal Compressors. *Orbit*. s.l. : Bently Nevada Corporation, 2000. Vol. 21, 1.
20. **International Electrotechnical Committee** Hydraulic Turbines, Storage Pumps and Pump-Turbines – Model Acceptance Tests *International Standard IEC 60193 BS EN 60193:1999*
21. **Dörfler, P.K, et al.** Stable Operation Achieved on a Single-Stage Reversible Pump-Turbine Showing Instability at No-Load. *Proceedings of the 19th IAHR Symposium on Hydraulic Machinery and Cavitation, Singapore*. 1998. págs. 431-440.
22. **Muszynska, Agnes.** whirl and whip-rotor/bearing stability problems. *Journal of sound and vibration*. 1986. Vol. 110, 3, págs. 443-462.
23. **Fan, Chen-Chao, et al.** Study of start-up vibration response for oil whirl, oil whip and dry whip. *Mechanical Systems and Signal Processing*. s.l. : Elsevier Ltd, 2011. 25, págs. 3102-3115. doi:10.1016/j.ymssp.2011.04.012.
24. **Braun, Olivier.** Part Load Flow in Radial Centrifugal Pumps. *PhD Thesis*. Lausanne : EPFL, 2009.